

A Data-Driven Electric Water Heater Scheduling and Control System

Gulai Shen, Zachary E. Lee, Ali Amadeh, K. Max Zhang*

Sibley School of Mechanical and Aerospace Engineering, Cornell University, Ithaca, NY 14853, USA

Abstract

Domestic hot water (DHW) heating accounts for up to 30% of average household energy use. Compared to gas fired water heaters, electric water heaters (EWH) can be powered by renewable generation resources, thus making it a potential renewable heating option. Furthermore, with the growing need for energy storage, incorporation of renewable resources, and initiatives worldwide, the electrification of DHW heating is expected to continue the rapid growth. However, many commercial EWH products with monitoring and alerting functionalities lack the intelligence to optimize and perform predictive control with data; on the other hand, research studies with refined models and simulations come short in incorporating real-time data and providing robust optimal controls under uncertainties in real-world settings. This paper presents a EWH Smart Scheduling and Control System using data-driven disturbance forecasts in a robust Model Predictive Control (MPC) to accomplish various demand side management objectives. Testing with a real-world EWH dataset and a two-state EWH model, prediction uncertainty is quantified and included in robust MPC simulations are conducted on a central EWH supplying DHW for a multi-unit apartment building. Results show that the proposed system is capable of anticipating DHW demand with an uncertainty interval covering up to 97% of the actual demand during the test days and reducing electricity cost up to 33.2% as well as maintaining a desired DHW temperature without affecting user comfort. Further, the flexibility of the system to alter load profiles under different Demand Response (DR) programs are demonstrated. Reductions in both power and gross consumption can be accomplished. The proposed system can create an implementable solution of forecasting DHW usage and optimizing controls as a part of a robust and reliable building energy management and control system in real-world settings.

1

2 Nomenclature

3 Δt Control time interval s

4 \dot{M}_w Hot water demand m^3/s

5 \dot{Q}_{demand} Heat loss due to demand of hot water W

6 \dot{Q}_{gen} Heat generation from power input W

7 \dot{Q}_{loss} Heat loss from water to ambient environment W

8 η Rated efficiency of water heater

*Corresponding author: kz33@cornell.edu

9	A	Surface area of water heater m^2
10	C_{off}	Off peak electricity price $\$/kWh$
11	C_{on}	On peak electricity price $\$/kWh$
12	c_p	Isobaric specific heat of water $kJ/(kgK)$
13	P	Rated power consumption of water heater W
14	Pe	Penalty during Demand Response period $\$/W$
15	Pe_1	Unit penalty for violation in magnitude of temperature $\$/^{\circ}C$
16	Pe_2	Unit penalty for violation in duration of time $\$/s$
17	Pe_{vio}	Comfort violation penalty $\$$
18	R	Thermal resistance of the water tank $(m^2K)/W$
19	S_i	State of water heater, binary on/off
20	T_a	Ambient temperature $^{\circ}C$
21	$T_{h,i}$	Hot water temperature at i th time step $^{\circ}C$
22	T_{ini}	Initial hot water temperature $^{\circ}C$
23	T_{in}	Supply domestic cold water temperature $^{\circ}C$
24	T_{low}	Lower limit of hot water temperature $^{\circ}C$
25	T_{up}	Upper limit of hot water temperature $^{\circ}C$
26	T_{vio}	Temperature magnitude violation $^{\circ}C$
27	t_{vio}	Time duration of violation s

28 1. Introduction

29 According to the 2015 Resident Energy Consumption Survey (RECS) [1], Domestic Hot Water
30 (DHW) provision consumes about 17.9 GJ of primary energy in the U.S., making it the second
31 largest end-use category in home energy use after space heating. The 2015 RECS also estimated
32 that around 16% of the average U.S. household's energy expenditure is for water heating. Apart
33 from energy consumption, DHW usage accounts for a sizable part of total water usage in residential
34 and commercial buildings. For example, an average person in North America uses around 64 liters
35 of hot water per day with typically higher usage during winters and lower usage during summers
36 [2].

37 Ranked by fuel types, natural gas, electricity (either through resistance heaters or heat pumps),
38 propane, and fuel oil are the main sources of energy for providing DHW [1]. With various initiatives
39 worldwide to decarbonize energy systems, the electrification of DHW heating is expected to continue
40 the rapid growth. In terms of energy management, a major advantage of electric water heaters
41 (EWHs) over fossil fuel-based options is that EWHs can be effectively integrated into the overall

42 building Demand Side Management (DSM), which has been shown to provide benefits such as peak
43 load reduction (peak shaving), lower electricity costs, and integration of intermittent renewable
44 energy resources. These DSMs can also incorporate or include flexible pricing structures and on-
45 site generation with additional capabilities to predict conditions and store energy. Thermal energy
46 stored in water storage tanks can decouple the demand for electricity and thermal power. There
47 are already more than 50 million electric water heaters (EWHs) in the U.S., comprising about 50%
48 of all water heaters in the country, which can provide a potential storage capacity of approximately
49 50 GWh [3]. With the built-in energy storage capability, EWHs have the potential to provide
50 services such as maximizing self-consumption of on-site renewable electricity generation, peak load
51 reduction (peak shaving), lowering electricity costs under dynamic or flexible pricing structures,
52 and integrating intermittent renewable energy resources into the power systems. DHW provision
53 systems are commonly designed so that more than enough hot water is always available to avert
54 comfort violations and the corresponding penalties that may be incurred. Thus, these systems may
55 experience significant energy loss without an accurate prediction of DHW usage. Moreover, a reliable
56 prediction of the DHW consumption profile over a control horizon is of paramount importance to
57 obtaining the optimal performance. So far, most of the existing DSM studies concerning EWHs have
58 been carried out based on artificially generated profiles with extensive statistical information [4–6].
59 The three yearly DHW demand profiles described by Jordan et al. [7] have been commonly used
60 in these studies. Nevertheless, when it comes to different buildings in real-life settings, the demand
61 behavior may vary significantly from one building to another and individual building behaviors
62 may not necessarily converge to the desired distribution. Thus, a data-driven approach with data
63 gathered on-site would be more reliable for predictions and further optimal control based on the
64 predictions.

65 When it comes to predicting DHW consumption, different factors need to be taken into consider-
66 ation. Region, culture, household size, and personal preferences are important contributing factors
67 in the hot water usage profile of a household [8], affecting peaks during morning and evening, dura-
68 tion of use, and average consumption. As mentioned earlier, the average DHW usage was estimated
69 at about 64 liters per person per day (LPD) for a U.S. household [2], while it was reported to be
70 around 43 LPD and 33 LPD for Finish and Swedish households, respectively [9, 10]. Forecasting
71 DHW can be targeted toward different sizes of households personal information may be required
72 and data acquisition can be very privacy intrusive especially for individual users. The problem also
73 becomes more of a human behavioral prediction problem [11]. While predicting the DHW consump-
74 tion of a multi-family dwelling can be essentially treated as a time series forecasting problem [12].
75 The approaches that deal with single and multi-family usage can be very different and approaches
76 developed can not be applied to or unable to generate satisfying results for both problems in general.

77 Different approaches can be found in the literature for predicting DHW consumption including
78 an analytical bottom-up approach [8], a feature specified bottom-up approach [13], and a statistical
79 approach with Autoregressive–Moving-Average (ARMA) [14, 15]. With the development of machine
80 learning algorithms, data-driven techniques for forecasting DHW consumption are becoming more
81 and more popular. Artificial Neural Network (ANN) [16], Recurrent Neural Network (RNN) [17],
82 and Reinforcement Learning [18] among others have been implemented for DHW consumption
83 predictions and demonstrated promising performance. Gelanzanskas and Gamage [19] compared
84 various DHW usage forecasting models and concluded that seasonal decomposition of the time-series
85 is of the utmost importance for obtaining accurate predictions.

86 In an EWH system scheduling problem, the main sources of uncertainty are associated with

hot water consumption prediction, ambient temperature, and cold water supply temperature over the planning horizon. It is worth noting that all the reviewed prediction approaches have their corresponding uncertainty levels, which need to be considered when formulating an optimization problem. Hong et al. [20] formulated an optimization problem to obtain the optimal temperature scheduling for an air-conditioning system which could be inspirational for other energy systems. As there existed uncertainty in the price and temperature predictions, they utilized fuzzy parameters for formulating the optimization problem. Thanks to the advances in robust optimization and optimization under uncertainty, different theories and methodologies can be used to take uncertainties into account in an optimization problem including probability theory [21], evidence theory, possibility theory, Bayes theory, and imprecise probabilities [22]. The most appropriate methodology for a given application should be selected considering data availability, uncertainty level, and problem complexity. Even though statistical models [23] or machine learning techniques [24] have proven their capabilities to model or quantify uncertainties, they have been rarely used water heating systems to develop stochastic or robust formulations for predictive control problems.

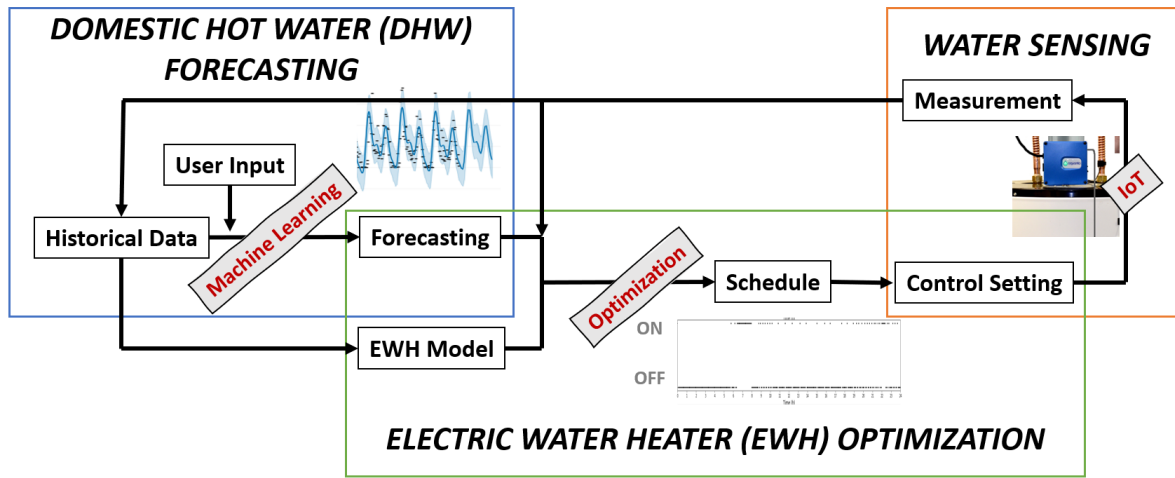


Figure 1: System design of the Electric Water Heater Smart Scheduling and Control System which consists of the Water Sensing that measures and stores data using Internet of Things (IoT) hardware and smart sensors, the DHW Forecasting that generates forecasting of hot water usage with machine learning algorithms from historical data, and the EWH Optimization that produces optimal schedules and controls for the EWH.

In an attempt to bridge the above-mentioned gap, this paper introduces a data-driven, predictive control scheme for optimizing the performance of an EWH system with the uncertainties taken into account. Unlike previous studies, real-life historical data has been used to formulate the robust optimization problem. The designed system, illustrated in Figure 1, consists of three main components named Water Sensing, DHW Forecasting, and EWH Optimization. The data obtained from the water metering is used to generate a forecast of the next day's DHW consumption profile. Combined with an EWH model, Model Predictive Control (MPC) simulations are performed to provide optimal control signals. Uncertainties in the DHW demand prediction are considered by specifying upper and lower bounds to ensure a robust control that brings financial savings for the consumer while maintaining thermal comfort. The performance of the system has also been investigated when participating in a demand response (DR) program. With all these features, the proposed system, referred to as Electric Water Heater Smart Scheduling and Control, has the potential to be integrated into real-world energy management systems to achieve the benefits of more intelligent control of electric water heating. While this paper focuses on the software and

115 algorithm side of the whole designed system, the designed IoT smart water meter which has the
 116 capability to measure water usage noninvasively is beyond the scope of this paper.

117 The rest of the paper is organized as follows. Section 2 outlines the methods and techniques
 118 employed for the proposed system. Section 3 presents and discusses the results obtained from the
 119 MPC simulations. Finally, Section 4 concludes the paper and provides recommendations for future
 120 work.

121 2. Methodology

122 The optimization problem formulated serves to achieve two main functions. First, it enables
 123 an optimized expected schedule for the next day EWH operation. It allows building operators and
 124 users to visualize the following day's operation and identify potential problems that might happen
 125 during some of the critical hours. Second, it is constantly resolved during the day to adjust and
 126 output the optimal control decisions. This allows the understanding of the current status of the
 127 system and future decisions based on what happened. It also allows the EWH to respond to various
 128 Demand Response programs or other emergency calls while still keeping the operation schedule
 129 close to optimal by minimizing cost and maintaining user comfort.

130 2.1. Control Model and Variables

131 With data and controls recorded and implemented every 5 minutes, the 24 hours of the planning
 132 horizon can be visualized in Figure 2. The system will solve for the optimized schedule of EWH
 133 over the whole remaining planning horizon with the initial conditions that are updated at each time
 134 step. Further, the nearest time step will take the action from the optimal schedule generated. The
 135 states of the EWH are calculated with an efficient EWH model in combination with data-driven
 136 predictions that will both be discussed in the following paragraphs.

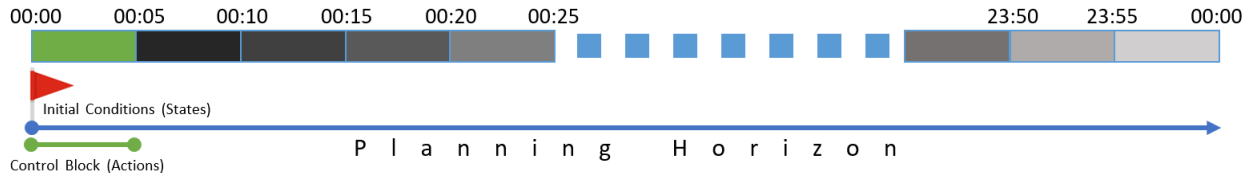


Figure 2: Planning horizon visualization with a day divided into 288 five minute intervals where flag represents the initial conditions.

137 2.2. Electric Water Heater Model

138 For the purpose of this paper, a fully mixed single-node EWH model is chosen since it is
 139 most computationally efficient and provides a reasonable confidence in making control decisions
 140 for EWHs. A Single-Node EWH model still is precise when the EWH is turned on for heating while
 141 precision drops when EWH is discharging water [25, 26]. Many existing works of control EWH sys-
 142 tems using a Single-Node model [27, 28] showed promising results. Admittedly, DHW use in terms
 143 of water flow might be affected by the differences in DHW temperature: a higher DHW setpoint
 144 might lead to reduced flow and volume usage with more cold water mixed. A better way of quan-
 145 tifying DHW use could be in terms of energy(enthalpy). Nevertheless, due to the limitation that
 146 the dataset does not gather DHW temperature data, volume usage is used for the prediction and
 147 modeling of EWH heat balances. The heat loss from the water mass to the ambient environment
 148 (W) can be modeled as:

$$\dot{Q}_{\text{loss}} = A(1/R)(T_h - T_a) \quad (1)$$

149 where A is the surface area of the water heater, R is the thermal resistance of the tank insulation,
 150 T_h is the hot water temperature inside the tank, T_a is the ambient temperature. In addition, the
 151 heat loss due to the demand for hot water can be modeled as:

$$\dot{Q}_{\text{demand}} = \dot{M}_w c_p (T_h - T_{\text{in}}) * 1000 \quad (2)$$

152 Where \dot{M}_w is the average hot water demand rate during the time interval, c_p is the isobaric specific
 153 heat capacity of water in , and T_{in} is the supply domestic cold water temperature. Lastly, the heat
 154 supplied from the EWH can be modeled as:

$$\dot{Q}_{\text{gen}} = P\eta S \quad (3)$$

155 where P is the power consumption, η is the efficiency of the electricity-to-heat transformation, S
 156 is the binary variable representing the on/off state of the water heater. The heat balance equation
 157 then can be derived as follows:

$$M c_p \frac{dT_h}{dt} = -\dot{Q}_{\text{loss}} - \dot{Q}_{\text{demand}} + \dot{Q}_{\text{gen}} \quad (4)$$

158 where M_w is the total mass of water stored in the water heater. An approximate solution can be
 159 obtained by taking the discrete average behavior over the 5 minute time interval of each control
 160 block to formulate a mixed integer linear programming problem. The governing equation for heat
 161 balance thus becomes:

$$(T_{h,i+1} - T_{h,i}) * M * c_p / \Delta t = -A(1/R)(T_{h,i} - T_a) - \\ \dot{M}_{w,i} c_p (T_{h,i} - T_{\text{in}}) * 1000 + P\eta S_i \quad (5)$$

162 The parameters used specifically in solving the governing equation are shown in Table 1. The
 163 specific parameters of the EWH can be set by referring to manufacturer documents or determining
 164 experimentally through data collection. In real-world settings, a data driven EWH would be desired
 165 since it would precisely fit each EWH in different conditions. The EWH used in this paper is a 950
 166 liter PVI Durawatt [29] commercial scale electric water heater. It is an EWH widely used in many
 167 multi-unit apartments with shared DHW supply. Electricity prices C_{on} and C_{off} are referenced from
 168 ConEd [30]. Further, the upper and lower limits of the DHW temperatures are set to avoid extreme
 169 high temperatures that could shorten the lifespan of components, preventing Legionnaires' disease,
 170 and complying local laws [31, 32].

171 2.3. Objectives and Settings

172 The objectives for many energy systems can vary from minimizing energy consumption, peak
 173 demand, or cost to maximizing user comfort or stability or a mix of both. For a EWH smart
 174 scheduling and control system addressed in this paper shown in Figure 1, it is important to have
 175 capabilities to adjust accordingly based on different types DSM. To show the capability of the
 176 system, two examples from Price-Based Program (PBP) and Incentive-Based Program (IBP) are
 177 chosen. From PBP, a Time of Use (ToU) tariff is chosen to be the objective for the problem to
 178 minimize the cost. Depending on the specific program chosen, ToU tariffs and demand charge may
 179 be considered. Thus, for a system modeled in this problem which only switches on and off with
 180 a constant power input, it is more reasonable to focus on the kWh cost. The chosen program for
 181 this paper is based on Consolidated Edison (ConEd) [30] PSC10-Class No.1 Rate II tariff shown in
 182 Figure 3.

Table 1: Parameters chosen in the optimization problem

Symbol	Meaning	Value
A	surface area, m^2	6
R	thermal resistance, $(m^2K)/W$	1
c_p	isobaric specific heat of water, $kJ/(kgK)$	4.18
P	nominal power of EWH, W	50000
η	efficiency of the EWH	0.95
M	mass of water in EWH, kg	946
T_{in}	input cold water temp, C	17
T_a	ambient temperature, C	17
C_{on}	on peak price (summer months), $$/kWh$	0.345
C_{on}	on peak price (other months), $$/kWh$	0.125
C_{off}	off peak price, $$/kWh$	0.0132
T_{up}	upper limit of DHW temp, C	72
T_{low}	lower limit of DHW temp, C	49
T_{ini}	initial temperature of DHW, C	52
Δt	control time interval, s	300

183 Regarding IBP, these programs normally require a coordinated reduction in energy use for all
 184 energy systems at demand side. While EWH alone plays a part of the overall electricity consumption
 185 for buildings, this smart scheduling and control system can be optimized and controlled to contribute
 186 to the overall reduction for the whole building. A high penalty can be added to the objective function
 187 during the DR period to motivate the EWH to be planned off and use its storage capacity to shift
 188 its load in advance. Once the DR call is received, normally with a minimal notice period of 1 to
 189 2 hours, the MPC can take in that information and modify the objective for the following EWH
 190 operation schedule.

191 The target multi-unit building chosen has about 130 residents in 60 units. The building has
 192 two PVI Durawatt electric water heaters with specifications described in Table 1. One EWH is
 193 the main one running with the other one as a backup. The EWH is also located in the basement
 194 with a stable room temperature. To generate the DHW use profile, we aggregate the data from 77
 195 individual EWHs given in [33]. This aggregated profile gives an example DHW usage behavior for
 196 a large population of residents that can be used to mimic a multi-family apartment building

197 2.4. Hot Water Demand Forecasting

198 The dataset used for this paper is reported in Refs. [33, 34]. The data is gathered from 77 electric
 199 water heaters over 120 days in South Africa. The days recorded are divided into four seasons with
 200 30 days for each season in the months of February, March, July, and September. Since South Africa
 201 is in the Southern Hemisphere, the coolest months are July and August while the warmest months
 202 are around January and February. The average temperature does not show a large variation over a
 203 typical year with lows around $45^{\circ}F$ to highs around $61^{\circ}F$. Data include both water use, ambient
 204 temperature, and power for each electric water heater at a frequency of 1 minute. This dataset
 205 is chosen because it gathers data for a large number of EWHs over an extended period of time,
 206 providing opportunities to compare both individual and aggregate behaviors. The dataset does
 207 provide multiple measurements for potential feature correlation analysis to understand how other
 208 factors might affect DHW usage, but the limited features provided motivate the forecasting to be

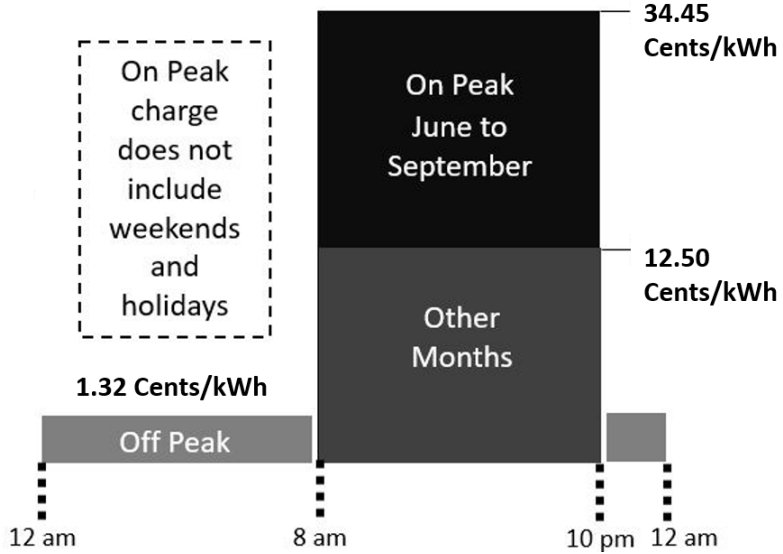


Figure 3: Consolidated Edison (ConEd) SC10-Class NO.1 Rate II Time of Use (ToU) tariff which is used to quantify electricity cost in this study.

209 a pure time series forecasting.

210 PROPHET [23] is employed for this DWH usage prediction problem. PROPHET is an open
 211 source software developed by Facebook that deals with common time series problems. Similar to
 212 ideas discussed by Gelanzanskas [19], PROPHET treats time series forecasting as a curve-fitting
 213 problem with the summation of multiple levels of curves:

$$y(t) = g(t) + s(t) + h(t) + \epsilon_t \quad (6)$$

214 Where the overall trend $g(t)$ is combined with seasonalities $s(t)$ from yearly, weekly, and daily levels
 215 in addition to the holiday effects $h(t)$ as well as noises ϵ_t extra conditional seasonality and regressor
 216 specified. Specifically, the model trend can be either a saturation growth model:

$$g(t) = \frac{C(t)}{1 + \exp(-k(t - m))} \quad (7)$$

217 or a piecewise linear model:

$$g(t) = (k + a(t)^T \delta)t + (m + a(t)^T \gamma) \quad (8)$$

218 depending on the training data with $C(t)$ being the time varying carrying capacity, k being the
 219 growth rate, and m being an offset parameter. To determine the change points in the trend, the
 220 rate of change is estimated with Maximum Likelihood Estimation (MLE) with a prior defined as a
 221 Laplace distribution. With a default value of 0.05, increasing the diversity parameter of the Laplace
 222 distribution can make the trend more flexible. Seasonalities are fitted using Fourier Series for the
 223 period effects with a stack of sine curves and a number of parameters that need to be estimated
 224 depending on the order of Fourier Series chosen:

$$s(t) = \sum_{n=1}^N a_n \cos\left(\frac{2\pi n t}{P}\right) + b_n \sin\left(\frac{2\pi n t}{P}\right) \quad (9)$$

225 Where n is the order of Fourier Series chosen and a_n and b_n are the parameters that need to be
 226 estimated. In this case, $P = 365.25$ is the interval length defined in Fourier Series for the yearly
 227 trend, and $P = 7$ is the interval length for the weekly trend. Holiday effects $h(t)$ are predefined
 228 with a list of U.S. holidays but can also be additionally specified. PROPHET also captures and
 229 predicts the uncertainty in both the overall trend, seasonalities, and additional observation noises.
 230 For uncertainty in the overall trend, it is assumed that the future change would replicate a similar
 231 rate as previously detected. By default, PROPHET samples 1000 points and sets an uncertainty
 232 interval of 80%. While for the uncertainty in seasonality, a generative model with full Bayesian
 233 Sampling using Monte Carlo Markov Chain technique can be defined to generate the uncertainty
 234 interval. This technique can be suitable for this problem to predict the aggregate behavior of 77
 235 EWHs to mimic a multi-family dwelling.

236 *2.5. Optimization and Robust MPC Formulation*

237 First to generate the optimal schedule through the planning horizon, an integer program assum-
 238 ing deterministic prediction can be formulated as below:

$$\begin{aligned}
 \min \quad & \sum_{i=1}^N C_i * P * S_i \\
 \text{s.t.} \quad & C_i = \begin{cases} C_{\text{on}} & \text{if during on-peak hours} \\ C_{\text{off}} & \text{if during off-peak hours} \end{cases} \\
 & T_{\text{low}} \leq T_{h,i} \leq T_{\text{up}} \\
 & (T_{h,i} - T_{h,i-1}) * M * c_p / \Delta t = -A(1/R)(T_{h,i-1} - T_a) - \\
 & \dot{M}_{w,i} c_p (T_{h,i-1} - T_{\text{in}}) * 1000 + P\eta S_i \\
 & T_{h,0} = T_{\text{ini}}
 \end{aligned} \tag{10}$$

239 Where the objective is to minimize electricity cost based on sample ToU tariff while making sure
 240 the temperature of the hot water is maintained between the limits and the heat balance of the hot
 241 water heater is satisfied. This basic formulation assumes a deterministic expected DHW demand
 242 in the future. Solving this optimization allows the visualization and understanding of the expected
 243 EWH behavior and electricity cost for the upcoming day.

244 To account for uncertainties from DHW forecasting, at each future time step, a range of the
 245 probable DHW consumption rates is calculated by PROPHET. The effects of a higher than predicted
 246 DHW consumption would lead to a greater value of heat loss, causing a lower than expected
 247 value of the DHW temperature inside the tank. On the other hand, a lower than expected DHW
 248 consumption would cause a higher than expected DHW temperature. Thus, when producing control
 249 outputs during the MPC simulations, it is important to make sure that the system is robust through
 250 these possible variations of future DHW consumption values at the upcoming time step. Based on
 251 this relationship, the uncertain DHW consumption can be modelled by modifying the temperature
 252 constraints in the optimization as follows,

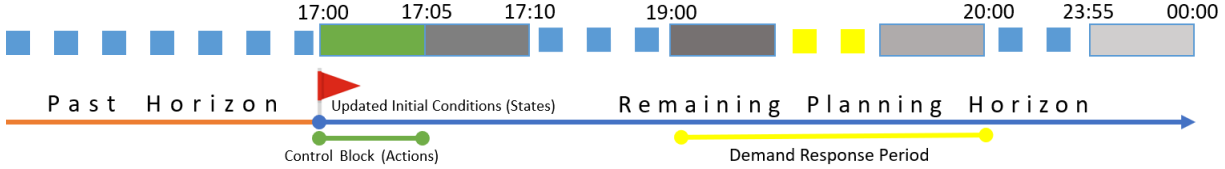


Figure 4: Planning horizon visualization with a DR notification received at 5pm for demand response period during 7pm to 8pm.

$$\begin{aligned}
 \min \quad & \sum_{i=1}^N C_i * P * S_i \\
 \text{s.t.} \quad & C_i = \begin{cases} C_{\text{on}} & \text{if during on-peak hours} \\ C_{\text{off}} & \text{if during off-peak hours} \end{cases} \\
 & T_{h,i} - ((\dot{M}_{w\text{ up},i-1} - \dot{M}_{w,i-1}) * c_p * (T_{h,i-1} - T_{in}) * \Delta t) / (M * c_p) \geq T_{\text{low}} \\
 & T_{h,i} + ((\dot{M}_{w,i-1} - \dot{M}_{w\text{ low},i-1}) * c_p * (T_{h,i-1} - T_{in}) * \Delta t) / (M * c_p) \leq T_{\text{up}} \\
 & (T_{h,i} - T_{h,i-1}) * M * c_p / \Delta t = -A(1/R)(T_{h,i} - T_a) - \\
 & \dot{M}_{w,i} c_p (T_{h,i-1} - T_{in}) * 1000 + P\eta S_i \\
 & T_{h,0} = T_{\text{ini}}
 \end{aligned} \tag{11}$$

253 As time propagates during the simulation, the initial temperature T_{ini} is updated from the EWH
 254 model while in real-life application, a temperature sensor is assumed to provide reliable feedback
 255 on the updated temperature.

256 Distribution Load Relief Program (DLRP) is an example of an emergence demand response pro-
 257 gram by ConEd. The program has a 2 hour notification period. An example of this program which
 258 notifies at 5pm for demand reduction during 7pm to 8pm is visualized in Figure 4. The objective
 259 function for the optimization is modified to add a penalty, acting like the potential incentive, for
 260 turning on the EWH during the DR period. Doing so would demotivate the EWH from turning
 261 on during this period of time and thus reduces both the average power and overall electricity con-
 262 sumption without jeopardizing thermal comfort. As a result, the robust optimization formulation
 263 is modified as follows,

$$\begin{aligned}
 \min \quad & \sum_{i=1}^N C_i * P * S_i + \sum_{j \in DR\text{ period}} P e_j * P * S_i \\
 \text{s.t.} \quad & C_i = \begin{cases} C_{\text{on}} & \text{if during on-peak hours} \\ C_{\text{off}} & \text{if during off-peak hours} \end{cases} \\
 & T_{h,i} - ((\dot{M}_{w\text{ up},i-1} - \dot{M}_{w,i-1}) * c_p * (T_{h,i-1} - T_{in}) * \Delta t) / (M * c_p) \geq T_{\text{low}} \\
 & T_{h,i} + ((\dot{M}_{w,i-1} - \dot{M}_{w\text{ low},i-1}) * c_p * (T_{h,i-1} - T_{in}) * \Delta t) / (M * c_p) \leq T_{\text{up}} \\
 & (T_{h,i} - T_{h,i-1}) * M * c_p / \Delta t = -A(1/R)(T_{h,i-1} - T_a) - \\
 & \dot{M}_{w,i} c_p (T_{h,i-1} - T_{in}) * 1000 + P\eta S_i \\
 & T_{h,0} = T_{\text{in}}
 \end{aligned} \tag{12}$$

264 In addition to the capability to optimize control schedules for the ToU tariff structure and

265 respond to DR programs, the system can also incorporate other price structures and energy sources
266 such as critical peak pricing and onsite solar generation. For example, dynamic pricing requires the
267 predictions of the electricity prices that can be accomplished with the similar methodology using
268 PROPHET and adding another uncertainty variable into the robust MPC formulations.

269 *2.6. Performance Evaluation*

270 To evaluate the performance of the control strategies, we quantify and compare two of the
271 most important factors for a demand-side user: electricity cost and user comfort. The cost can
272 be calculated by the actual schedule of EWH through the simulations and compared to a baseline
273 situations. In this paper, the baseline is constructed based on a thermostatic control, namely a
274 simple and widely used rule-based temperature control method which maintains the temperature
275 within the upper and lower limits. Evaluating the performance of the system with regard to thermal
276 comfort needs further analysis. In some states in the US such as New York, it is required for
277 residential buildings to provide DHW with a minimum temperature of $120^{\circ}F$ always. Building
278 management companies could be subject to significant fines and penalties starting from \$250 per
279 day [32]. Nevertheless, the rules normally get relaxed as a minor deficiency in temperature for a
280 short period of time is typically tolerable. Thus, to evaluate the performance, a 95% fulfillment
281 limit is set. If DHW temperature is maintained above $120^{\circ}F$ for over 95% of the time during the
282 day, the following minor penalty would be applied based on the average temperature violation and
283 the duration of violation with unit penalties of Pe_1 and Pe_2 :

$$Pe_{vio} = Pe_1 * \overline{T_{vio}} + Pe_2 * t_{vio} \quad (13)$$

284 where T_{vio} is the temperature of violation and t_{vio} is the duration of violation. If the fulfillment
285 time drops below 95%, it would be considered a major violation which is not tolerable and would
286 incur the large penalties.

287 For DR program in New York State specifically, there exists a large variety of criteria designed
288 and enforced by wholesale power system operators and energy suppliers like New York Independent
289 System Operator (NYISO) and ConEd. To calculate the demand reduction for a DR program, the
290 normal procedure is to calculate the Customer Base Load based on recorded usage from previous
291 days with adjustments [35, 36]. Thus, to evaluate how well the EWH responds to the overall building
292 demand reduction call, the average base load is calculated by generating the anticipated schedules
293 over past days and then compared to the actual load during the day with a DR call.

294 **3. Results and Discussion**

295 *3.1. Domestic Hot Water Forecasting*

296 *3.1.1. Dataset Analysis and Visualization*

297 Considering DHW usage over 30 days for one EWH from the dataset, a recognizable pattern
298 can be observed for individual DHW usage with a larger peak with shorter duration in the morning
299 and a lower peak with longer duration in the evening. While the duration of DHW use is similar
300 in different seasons, the average daily DHW use takes a higher value in winter and a lower value in
301 summer. Specifically, winter has the highest average daily DHW use of 23.8 L, following by spring
302 of 20.9 L, fall of 17.2 L, and summer of 16.8 L. This proves seasonal variation of household's DHW
303 use with 41.7 % increase from warmer months to cooler months.

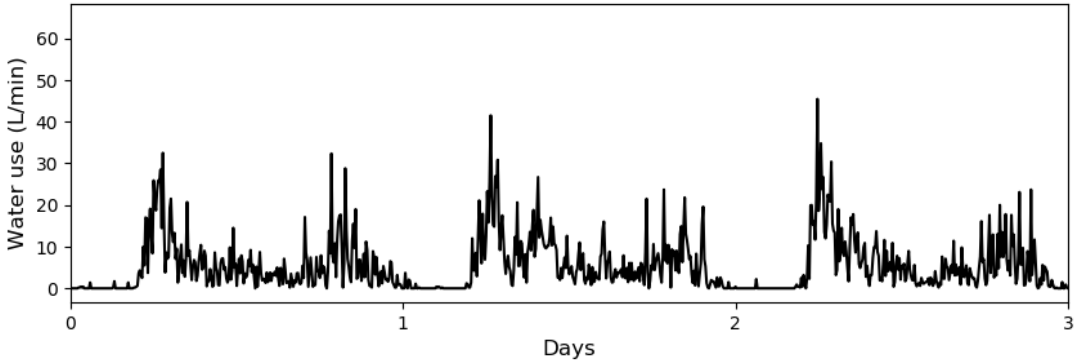


Figure 5: Aggregated pattern of 77 EWHs for three example days.

304 A correlation analysis of the dataset shows that DHW use is relatively independent of outdoor
 305 air temperature, with a correlation coefficient of 0.004. This is mainly because the dataset is pro-
 306 vided with one month for each season preventing year-long training data to show the continuous
 307 seasonal variations. With one month of data used for each season, in addition to the well-maintained
 308 indoor temperature, the correlation is thus low and neglectable on a sub-hourly basis. The seasonal
 309 variation can be better understood when comparing the daily usage versus the daily average tem-
 310 perature. These two variables show a moderate correlation of 0.23. Further, the average seasonal
 311 usage numbers are much more convincing on proving the seasonal variations discussed in the fol-
 312 lowing paragraph. Thus, ambient temperature is not included in the DHW forecasting model which
 313 aims to predict sub-hourly usage of DHW, leading to a pure time-series treatment of the DHW
 314 forecasting with this dataset.

315 In order to use the data to mimic a multi-dwelling apartment complex, the data from the 77
 316 individual EWHs is aggregated as shown in Figure 5 for 3 typical days in the summer season. The
 317 aggregated data also shows a more recognizable daily pattern for multi-family dwellings [37]. The
 318 aggregated data shows the daily average usages for different seasons to be 7670.9 L for summer,
 319 7821.6 L for fall, 10850.1 L for winter, and 9522.97 L for spring, leading to a daily average use of
 320 8966.4 L over the year. Comparing to the 130 resident target building in the U.S. with 64 liters
 321 per day per person usage, the dataset can well represent the usage in the target building with a
 322 discrepancy less than 10%. Thus, the aggregated profile will be used for training and testing the
 323 model.

324 3.1.2. Forecast Generations

325 The forecasts were generated using PROPHET and are shown in Figure 6. The black dots
 326 represent the training data while the grey line represents the fitted curve and the predicted values
 327 of the following day and the grey shades represent the uncertainty range. Ideally in real-world
 328 settings, over a year of data would be desired to capture more patterns. The package generates
 329 multiple plots for visualization in Figure 7. It shows how PROPHET’s additive model works by
 330 adding up (a) the overall model trend defined as a piecewise linear model, (b) the daily and (c)
 331 the weekly seasonalities fitted with Fourier Series curves, and (d) the extra morning and evening
 332 regressors. When predicting demand at one timestamp into the future, the trend is assumed to be
 333 maintained with possible changepoints sampled randomly. In addition to the time of day value,
 334 day of week, and morning and evening regressor values summed. From Figure 7, the training data
 335 shows the most obvious pattern for the daily seasonality with the morning and evening peaks. If
 336 more data were gathered in the future, the seasonal behavior change of DHW demand and better

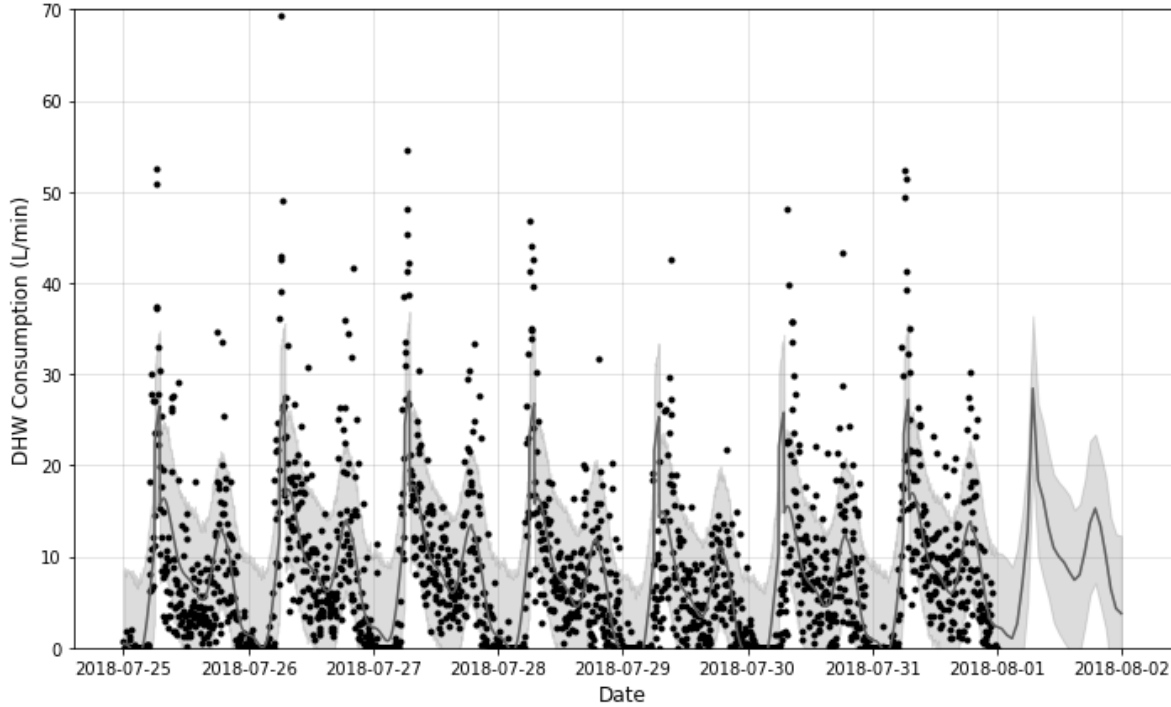


Figure 6: PROPHET prediction visualization.

337 weekly seasonalities can be expected. Further, with the incorporation of the morning and evening
 338 regressors, the "outlier" points that are filtered out by the daily seasonality curve got preserved to
 339 provide better predictions.

340 The forecasting result of a test summer day is shown in Figure 8 together with the actual DHW
 341 profile, and the upper and lower limits. It can be observed that the overall trend of the DHW profile
 342 is well captured and the fluctuation of the actual DHW consumption can be well covered within
 343 the upper and lower limits of the prediction while a few peaks are not fully covered. Note that, the
 344 seasonality profiles based on Fourier Series tend to smooth out the high morning and evening peaks
 345 and consider them as outliers. To better predict and incorporate these values into the possible range,
 346 additional regressors are added during the morning and evening peak times. The addition of the
 347 extra regressor significantly helps with producing an uncertainty interval that covers the variations
 348 in the actual values. Changing the uncertainty interval does impact the width of the upper and
 349 lower limits due to the sampling method that PROPHET uses. A proper uncertainty interval should
 350 maintain the robustness of the system while not affecting energy and cost savings. These results
 351 provide a good foundation for the following optimization of the EWH control schedules and model
 352 predictive control simulations. PROPHET's Python API also makes integration seamlessly with
 353 further data manipulation as well as optimization.

354 *3.2. Electric Water Heater Optimal MPC Simulation*

355 Optimizing the schedule for the EWH with a Mixed-Integer Programming formulation is a NP-
 356 Complete problem that requires extensive computing resources and time to get an optimal solution.
 357 A one day ahead optimal schedule can be generated by solving the optimization problem once.
 358 Furthermore, by solving the optimization repeatedly over the receding horizon, the optimal controls
 359 can be generated. Though global optimum is not guaranteed by the solution presented since the
 360 optimality gap does not necessarily converge to zero, only the first control signal is applied to the

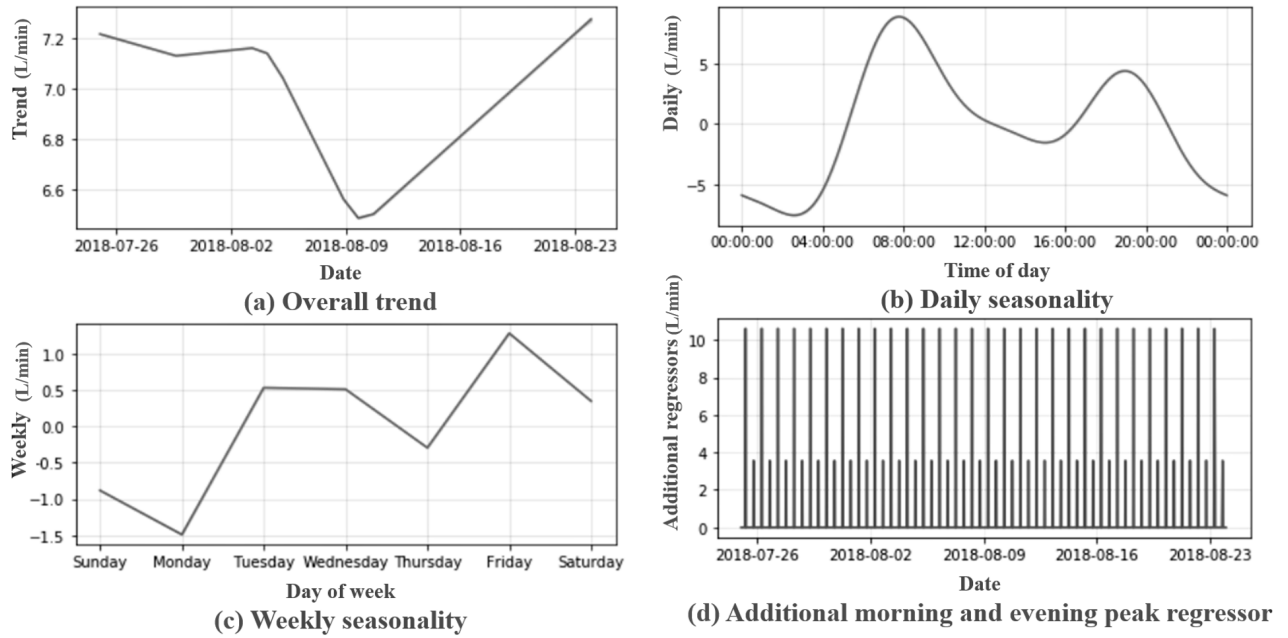


Figure 7: (a) Overall trend, (b) daily seasonality, (c) weekly seasonality, and (d) additional morning and evening peak regressors for the additive model that generates the resulted forecast.

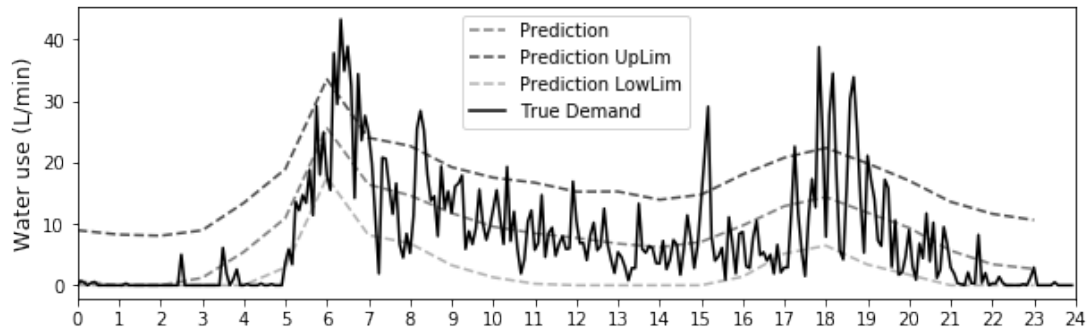


Figure 8: PROPHET prediction for one summer day.

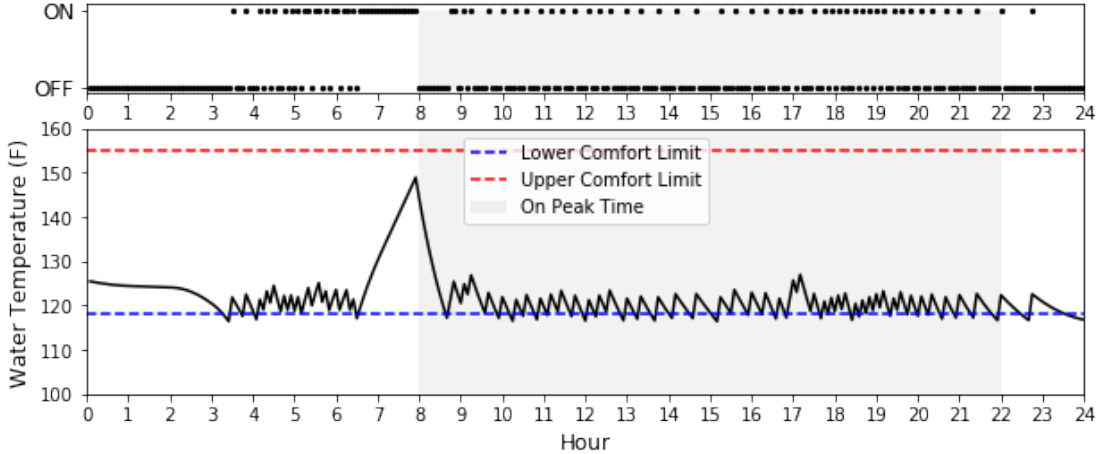


Figure 9: Optimal schedule of the EWH state and DHW temperature for one summer test day.

361 system. The continuously running MPC will repeatedly take in new information about the latest
 362 state of the system and generate a new optimal schedule for the remaining period of time.

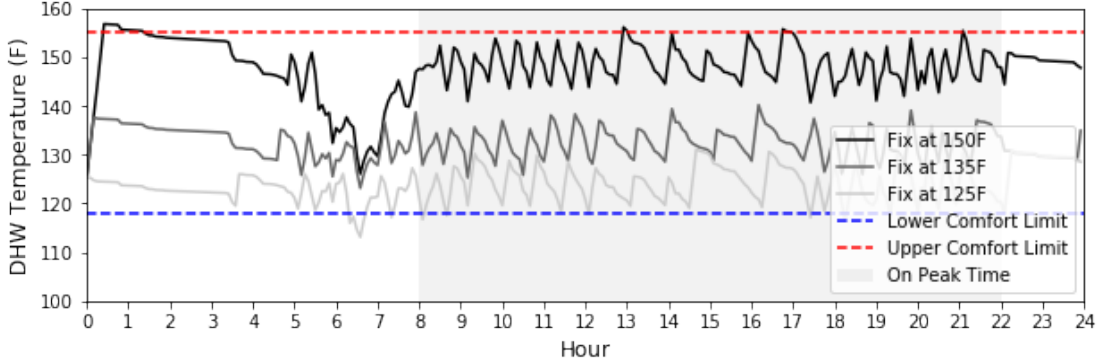
363 *3.2.1. ToU (PBP) simulation and Performance*

364 Using the predictions generated, Figure 9 shows the optimized schedule with the predicted
 365 hot water demand as a single deterministic value at each time step. The optimized schedule is
 366 minimizing the electricity cost based on the ToU tariff structure chosen with a higher electricity price
 367 from 8am to 10pm. The top subplot shows the on/off state of the EWH while the bottom subplot
 368 shows the anticipated DHW temperature inside the EWH. Repeating the process for optimizing a
 369 winter day, the expected electricity costs are \$68.06 and \$38.76 respectively.

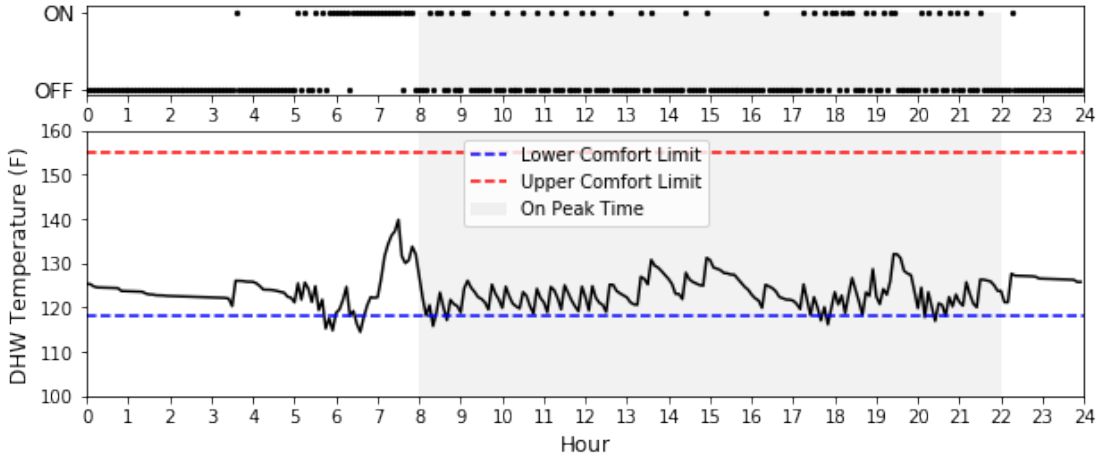
370 Observing the results from the optimal day ahead schedules, a period of preheating the water
 371 before 8am can be seen. The water temperature is raised to around 60°C (140°F) which is much
 372 higher than the desired DHW temperature normally set at 49°C (120°F). In this case, because the
 373 objective is set to minimize electricity cost under a ToU tariff, the behavior of preheating happens
 374 right before when electricity price increases drastically. This allows heat energy to be generated
 375 at a lower cost and be stored for future demand. Afterward, during the on-peak period, the main
 376 behavior of the EWH is to remain close to the lower bound of water temperature of 49°C (120°F)
 377 in order to minimize the electricity cost. The expected electricity cost can be calculated and shown
 378 at the beginning of the day as a reference. Solving this optimization problem also outputs the next
 379 control action of the EWH as one step of the MPC simulation. By solving the optimization problem
 380 repeatedly as new measurements are feedback to the system, the system is able to determine the
 381 following control actions.

382 Conventional thermostatic control, an example of heuristic or rule-based control, tries to main-
 383 tain a constant temperature set-point of DHW with a small range of variation. The system is
 384 controlled in response to demand: turn on the EWH if the lower limit temperature is reached, turn
 385 off EWH if the upper limit temperature is reached. One of the easiest Demand Side Management
 386 for households is actually to lower the DHW temperature set point. While Lowering DHW temper-
 387 ature can save a significant amount of energy, risk of being unable to meet the demand increases
 388 which could affect user comfort and cause high penalties.

389 Shown in Figure 10a are the expected behaviors of the EWH with DHW temperature set at



(a) Simulation for rule-based thermostatic control of EWH over one summer test day at different set-point temperature.



(b) Simulation for MPC of EWH state and DHW temperature over one summer test day.

Figure 10: Simulation for different control methods for EWH over one summer test day where (a) simulates the DHW temperature under rule-based thermostatic control and (b) simulates the EWH state and DHW temperature under MPC.

around 66°C (150°F), 57°C (135°F), and 52°C (125°F) on the summer test day. Respectively, setting DHW at lower temperatures generates 17.0% and 29.1% savings in electricity cost compared to a fixed set-point above 66°C (150°F). Note that these control strategies are purely responsive to the previous time step's demand and have a high probability to run out of hot water if the EWH is not properly sized or a high demand is expected in the future. Thus, normally to avoid the violations, temperatures are set to a higher value. In both of the cases where DHW set points are 66°C (150°F) and 57°C (135°F), no violation occurs. While setting the temperature at 52°C (125°F), 15 minutes of average violation of 2°F occurred, dropping the fulfillment range to 99.0%. Figure 10b shows how could an EWH behave with prediction and MPC. Similar to the previously shown day-ahead schedule, the MPC simulation shows a preheating before 8am to utilize the lower electricity charges. In addition, because MPC constantly takes in updated temperature values while re-optimizing, the violation time is reduced to only 5 minute with an average of 1°C (1.8°F). Listed in Table 2, MPC method generates 33.2% savings over the base cost with conventional control by maintaining water at 66°C (150°F).

Repeating the process for the winter test day, the results are plotted in Figure 11a and the electricity costs simulated are shown in Table 3. Compared to the base case of conventional control, the reductions in electricity cost are 16.3%, 28.2% and 28.0% respectively. Note that due to the

Table 2: Electricity costs and comfort fulfillment comparison for one summer day simulation with different control methods.

	Electricity Cost	Reduction	Fulfillment
Fixed @66°C (150°F)	\$85.23		100%
Fixed @57°C (135°F)	\$70.71	17.0%	100%
Fixed @52°C (125°F)	\$60.44	29.1%	99.0%
MPC	\$59.00	33.2%	99.7%

Table 3: Electricity costs and comfort fulfillment comparison for one winter day simulation with different control methods.

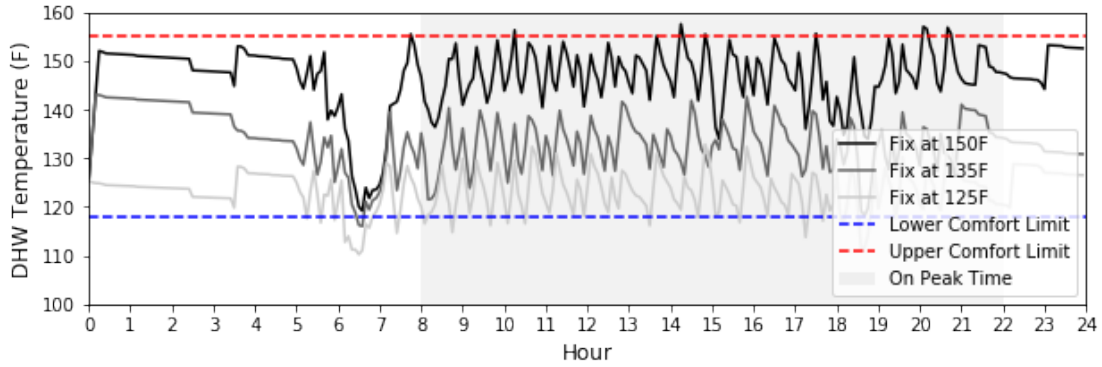
	Electricity Cost	Reduction	Fulfillment
Fixed @66°C (150°F)	\$57.38		100%
Fixed @57°C (135°F)	\$48.02	16.3%	99.0%
Fixed @52°C (125°F)	\$41.22	28.2%	94.4%
MPC	\$41.35	28.0%	98.3%

407 higher DHW demand, the high morning peak causes the temperature to drop significantly below
 408 the set-points for conventional control methods if the temperature settings are too low. In this
 409 test example, if DHW temperature is set at around 49°C (120°F), there would be 80 minutes of
 410 violation of average 2°C (4°F) which makes the fulfillment rate drop below the 95% limit. Thus,
 411 it is expected to cause significant penalties and this control strategy is not desired. If MPC is used
 412 as the control method shown in Figure 11b, the violation time is significantly reduced due to the
 413 presence of DHW demand prediction while the electricity cost is still reduced by 28% compared to
 414 the baseline case. The result shows the capability of MPC to provide energy cost reduction and
 415 maintain user comfort when conventional controls are unable to achieve both objectives.

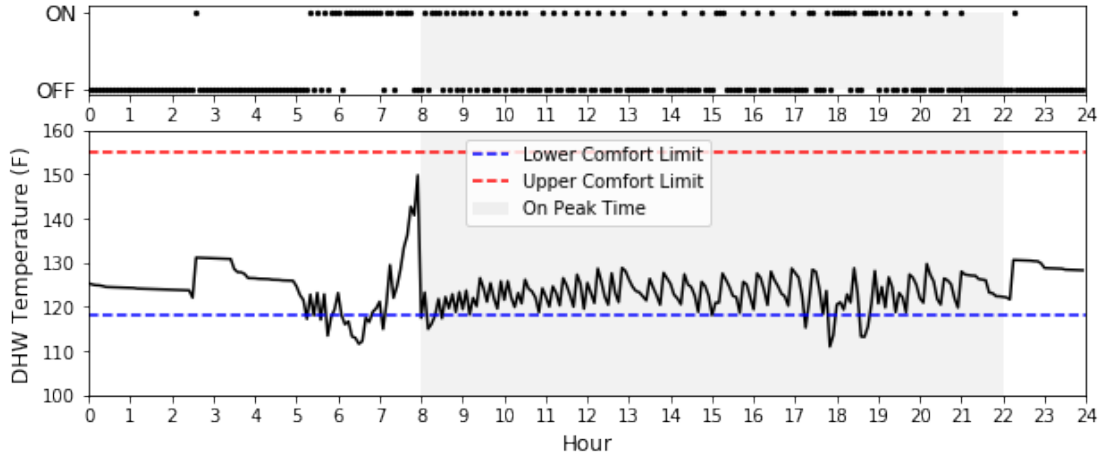
416 Performing an extended simulation over six test days, the results are shown in Figure 12. The
 417 baseline conventional controls with fixed DHW set-points are also plotted. The results for cost
 418 reduction and user comfort fulfillment are shown in Table 4. On average, 29.7% reduction in
 419 electricity cost and 98.9% user comfort fulfillment can be achieved. Consistently, MPC is reliable
 420 and efficient to reduce electricity cost and maintain user comfort.

Table 4: Electricity costs reduction and comfort fulfillment over six days of MPC simulation compared with rule-based thermostatic control simulation.

	Cost Reduction	Fulfillment Improvement	Fulfillment
Summer Day1	29.7%	1.8%	98.6%
Summer Day2	30.0%	2.9%	99.7%
Summer Day3	33.2%	0.7%	99.7%
Winter Day1	28.3%	2.5%	99.0%
Winter Day2	29.0%	2.2%	98.0%
Winter Day3	28.0%	3.9%	98.3%
Average	29.7%	2.3%	98.9%



(a) Simulation for rule-based thermostatic control of EWH over one winter test day at different set-point temperature.



(b) Simulation for MPC of EWH state and DHW temperature over one winter test day.

Figure 11: Simulation for different control methods for EWH over one winter test day where (a) simulates the DHW temperature under rule-based thermostatic control with a set point temperature at $66^{\circ}C$ ($150^{\circ}F$) and (b) simulates the EWH state and DHW temperature under MPC.

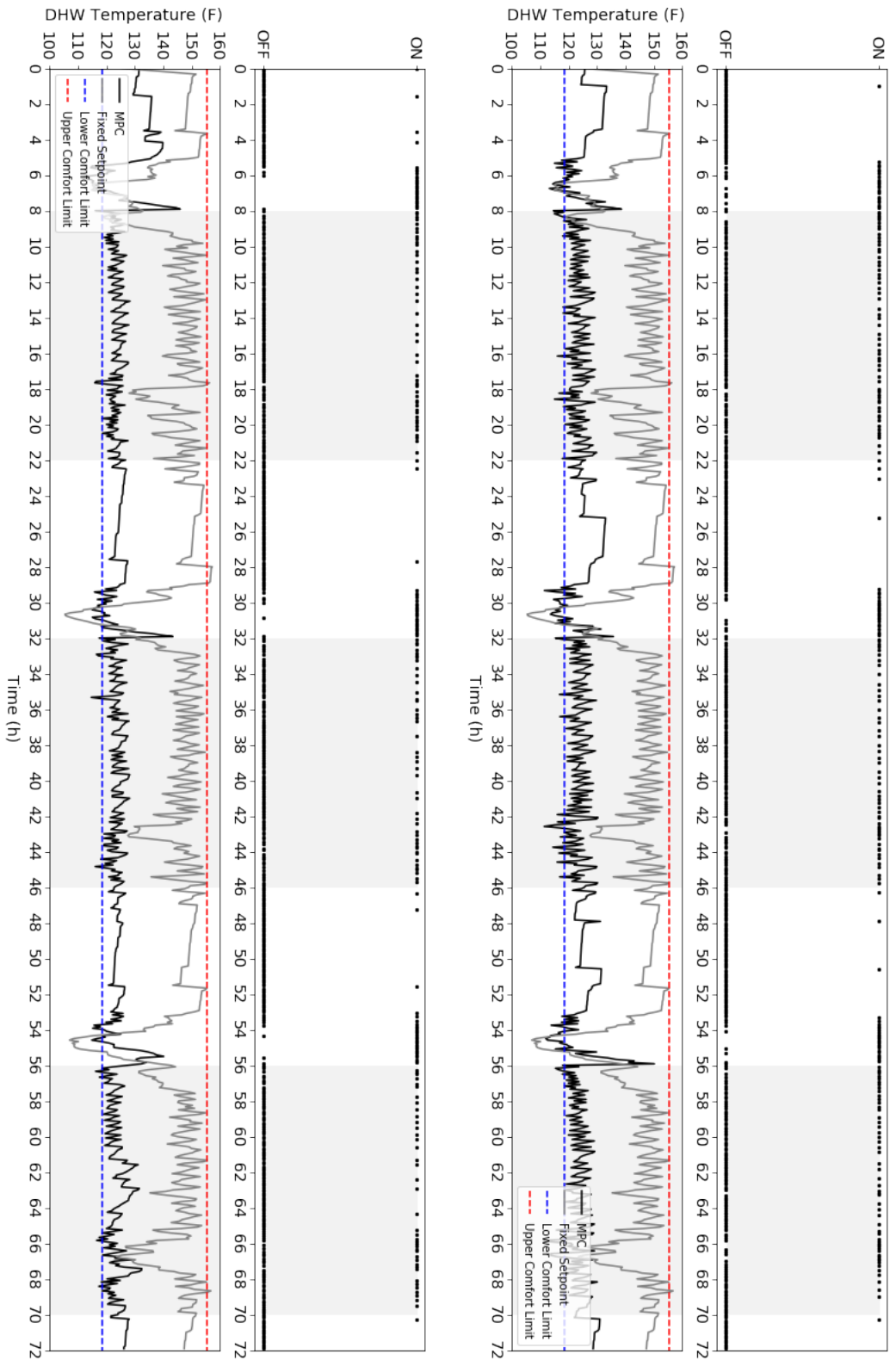


Figure 12: Left: Simulation of EWH state and DHW temperature over three summer test day using thermostatic control and MPC. Right: Simulation of EWH state and DHW temperature over three winter test day using thermostatic control and MPC.

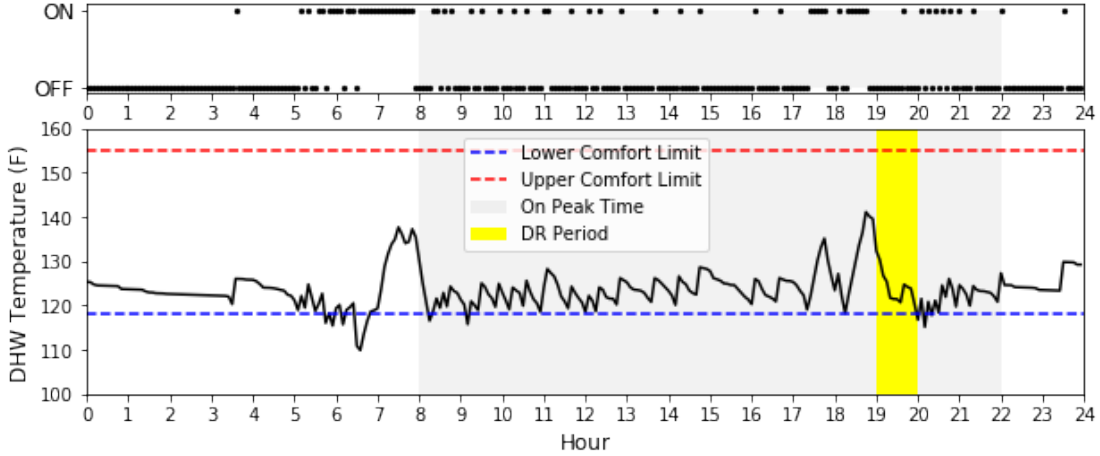


Figure 13: Adjusted schedule of EWH state and DHW temperature for demand response program notifying at 5pm and happening during 7pm to 8pm.

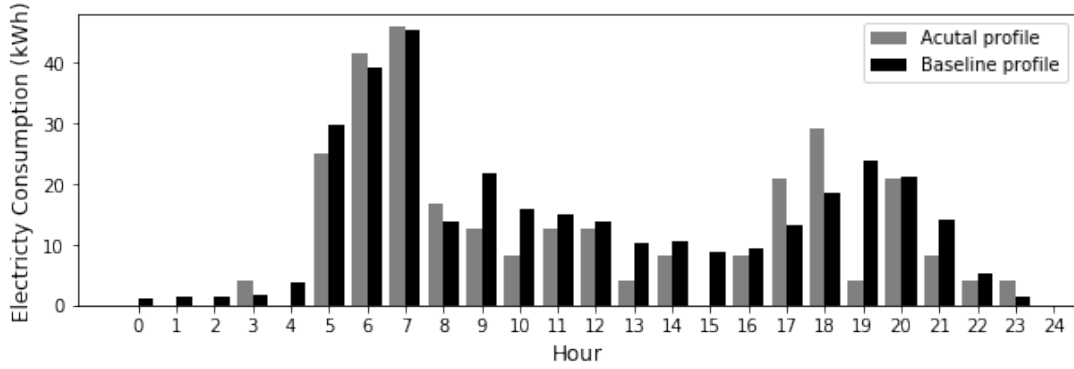


Figure 14: Comparison between the summer baseline load profile and the actual optimally adjusted load profile with demand reduction between 7pm to 8pm.

3.2.2. Demand Response(IBP) Simulation and Performance

Simulating a DR call made at 6pm for a demand reduction from 7pm to 8pm, the schedule will be instantly adjusted accordingly and the result is shown in Figure 13. With the modified objective, the EWH is planned to be off during this one hour period. Even though raising DHW temperature during the on-peak period may cause excessive heat loss and higher tariff, the EWH turns on to heat the water before 7pm to generate enough storage for the use during the DR period.

To quantify the reduction in both average power and gross consumption, a baseline hourly load profile needs to be constructed first. Shown in Figure 14, the consumption based on the optimized schedules of 20 previous days in the summer are calculated and divided into hourly profile and the actual load profile for the day with a DR call during 7pm to 8pm. A reduction of 19.66 kWh of electricity can be achieved during the DR period. Thus, for the whole building system, a reduction in average power during the DR period contributed by the EWH system can be expected as well.

4. Conclusion

This paper presents a part of the closed loop electric water heater (EWH) smart scheduling and control system with forecast and robust model predictive control algorithms. The objective is to

436 create an implementable solution of forecasting usage and optimizing controls as a part of a robust
437 and reliable smart building energy management and control system in real-world settings.

438 To achieve these, an EWH dataset containing data for over 120 days of DHW usage from
439 77 EWHs gathered at one minute frequency is chosen to demonstrate the methods and results.
440 PROPHET [23] is used for DHW forecasting with a quantified uncertainty range. Results both
441 capture the overall trend and cover the actual usage profile with the uncertainty interval well. A
442 mixed-integer linear programming problem is formulated using a fully mixed single node EWH
443 model to solve for the optimal schedule over the planning horizon and the following control actions
444 with the flexibility to alter between different objectives based on energy programs enrolled. Simu-
445 lation shows up to about 30% electricity cost reductions over 6 test days with an average comfort
446 fulfillment rate of about 99%. Simulation also shows the capability to shift load profile for reducing
447 average power and gross consumption on short notice. On an example summer day with a demand
448 response (DR) call, testing with a constructed baseline load profile, a reduction of about 20 kWh
449 of electricity is observed during the demand response period.

450 DHW demand data, while currently very limited, can go a long way in improving EWH control
451 efficiency. By using real data instead of artificially generated demand profiles, our data-driven
452 approach can capture more realistic operating conditions and can be tuned to each building's specific
453 DHW demand behavior. However, measuring volumetric flow, as in the presented dataset, may not
454 be completely sufficient for determining DHW demand in all cases. While in most cases the discharge
455 temperature remains relatively constant, large DHW draws can sometimes lower this temperature,
456 resulting in a higher volume draw to maintain the same enthalpy draw. Thus, data containing
457 additional measurements that determine enthalpy demand may provide a more complete model
458 of DHW demand. Moreover, implementation can require additional ongoing research topics such
459 as hardware and sensor installation, performing state estimation, and reducing the computational
460 burden.

461 There are also several potential extensions of this work, including the incorporation of onsite
462 generations from photovoltaic systems, day-ahead and real-time electricity pricing, and other more
463 complex and flexible systems and variations[38]. While the general methodology that accounts for
464 uncertainty remains similar to that proposed in this paper, additional modifications to the objective
465 function and system model could expand the potential control objectives. Finally, while this system
466 is designed for aggregated multi-family DHW control, more complex prediction algorithms that can
467 achieve the significantly more difficult task of predicting single-family DHW demand could allow
468 this methodology to provide efficient single-family DHW control as well.

469 Acknowledgments

470 The authors acknowledge the support from the National Science Foundation (NSF) under grant
471 1711546 and the NSF Graduate Research Fellowships Program (to ZEL). The authors also would
472 like to acknowledge Professor Fengqi You at Cornell University for the advice and inspiration on
473 the development of the topic and content of this paper.

474 References

475 [1] Space heating and water heating account for nearly two thirds of U.S. home energy use, U.S.
476 Energy Information Administration, 2018.

477 [2] D. S. Parker, P. W. Fairey, J. D. Lutz, Estimating daily domestic hot-water use in north
478 american homes, *ASHRAE Trans* 121 (2015).

479 [3] Residential Energy Consumption Survey (RECS), U.S. Energy Information Administration,
480 2017.

481 [4] D. Vanhoudt, D. Geysen, B. Claessens, F. Leemans, J. L., J. Van Bael, An actively controlled
482 residential heat pump: Potential on peak shaving and maximization of self-consumption of
483 renewable energy, *Renewable Energy* 63 (2014) 531 – 543.

484 [5] R. De Coninck, R. Baetens, D. Saelens, A. Woyte, L. Helsen, Rule-based demand-side man-
485 agement of domestic hot water production with heat pumps in zero energy neighbourhoods,
486 *Journal of Building Performance Simulation* 7 (2014) 271–288.

487 [6] P. Kepplinger, G. Huber, J. Petrasch, Autonomous optimal control for demand side man-
488 agement with resistive domestic hot water heaters using linear optimization, *Energy and*
489 *Buildings*, 100 (2015) 50–55.

490 [7] U. Jordan, K. Vajen, Realistic domestic hot-water profiles in different time scales, Report for
491 IEA-SHC Task 26 (2001).

492 [8] A. Ferrantelli, K. Ahmed, P. Pylsy, J. Kurnitski, Analytical modelling and prediction formulas
493 for domestic hot water consumption in residential Finnish apartments, *Energy and Buildings*
494 143 (2017) 53–60.

495 [9] K. Ahmed, P. Pylsy, J. Kurnitski, Monthly domestic hot water profiles for energy calculation
496 in Finnish apartment buildings, *Energy and Buildings* 97 (2015) 77 – 85.

497 [10] Boverket, Regelsamling för byggande (Collection of rules for construction), BBR 2012,
498 <https://bit.ly/39uCPqP>, 2012.

499 [11] S. Cao, S. Hou, L. Yu, J. Lu, Predictive control based on occupant behavior prediction for
500 domestic hot water system using data mining algorithm, *Energy Science & Engineering* 7
501 (2019) 1214–1232.

502 [12] J. G. DeGooijer, R. J. Hyndman, 25 years of time series forecasting, *International Journal of*
503 *Forecasting* 22 (2006) 443 – 473.

504 [13] H. Aki, T. Wakui, R. Yokoyama, Development of a domestic hot water demand prediction
505 model based on a bottom-up approach for residential energy management systems, *Applied*
506 *Thermal Engineering* 108 (2016) 697 – 708.

507 [14] A. Lomet, F. Suard, D. Chèze, Statistical modeling for real domestic hot water consumption
508 forecasting, *Energy Procedia* 70 (2015) 379 – 387. International Conference on Solar Heating
509 and Cooling for Buildings and Industry, SHC 2014.

510 [15] D. Popescu, E. Serban, Simulation of domestic hot-water consumption using time-series mod-
511 els, in: *Proceedings of the 6th IASME/WSEAS International Conference on Heat Transfer,*
512 *Thermal Engineering and Environment*, Rhodes, Greece, 2008, pp. 20–22.

513 [16] A. Delorme-Costil, J. Bezian, Forecasting domestic hot water demand in residential house
 514 using artificial neural networks, in: 2017 16th IEEE International Conference on Machine
 515 Learning and Applications (ICMLA), 2017, pp. 467–472.

516 [17] Y. Qin, D. Song, H. Cheng, W. Cheng, G. Jiang, G. W. Cottrell, A dual-stage attention-based
 517 recurrent neural network for time series prediction (2017). Proceedings of the Twenty-Sixth
 518 International Joint Conference on Artificial Intelligence (IJCAI-17).

519 [18] H. Kazmi, S. D’Oca, C. Delmastro, S. Lodeweyckx, S. P. Corgnati, Generalizable occupant-
 520 driven optimization model for domestic hot water production in NZEB, Applied Energy 175
 521 (2016) 1 – 15.

522 [19] L. Gelazanskas, K. A. A. Gamage, Forecasting hot water consumption in residential houses,
 523 Energies 8 (2015) 12702–12717.

524 [20] Y. Y. Hong, J. K. Lin, C. P. Wu, C. C. Chuang, Multi-objective air-conditioning control
 525 considering fuzzy parameters using immune clonal selection programming, IEEE Transactions
 526 on Smart Grid, 3(4) (2010) 1603–1610.

527 [21] D. Bertsimas, V. Gupta, N. Kallus, Data-driven robust optimization, Mathematical Program-
 528 ming, 167(2) (2017) 235–292.

529 [22] A. Messac, Optimization in Practice with MATLAB, Combridge University Press, 2015.

530 [23] S. Taylor, B. Letham, Forecasting at scale, The American Statistician 72 (2018) 37–45.

531 [24] C. Shang, F. You, A data-driven robust optimization approach to scenario-based stochastic
 532 model predictive control, Journal of Process Control 75 (2019) 24 – 39.

533 [25] O. Dumont, C. Carmo, R. Dickes, E. Georges, S. Quoilin, V. Lemort, Hot water tanks: How
 534 to select the optimal modelling approach?, in: CLIMA 2016 Aalborg, Denmark, 2016.

535 [26] A. L. Nash, A. Badithela, N. Jain, Dynamic modeling of a sensible thermal energy storage
 536 tank with an immersed coil heat exchanger under three operation modes, Applied Energy 195
 537 (2017) 877 – 889.

538 [27] A. Sepulveda, L. Paull, W. G. Morsi, H. Li, C. P. Diduch, L. Chang, A novel demand side man-
 539 agement program using water heaters and particle swarm optimization, 2010 IEEE Electrical
 540 Power and Energy Conference (2010).

541 [28] L. Paull, H. Li, L. Chang, A novel domestic electric water heater model for a multi-objective
 542 demand side management program, Electric Power Systems Research, 80(12) (2010) 1446–1451.

543 [29] PVI, Durawatt ASME Electric Storage Water Heater, <https://bit.ly/39wbbKo>, 2018.

544 [30] Consolidated Edison, Schedule for Electricity Service PSC10-Class No. 1 Rate II,
 545 <https://bit.ly/2EmnoFT>, 2012.

546 [31] Miller, T. and Yuko, E., What is the best temperature for my water heater?,
 547 <https://lifehacker.com/whats-the-best-temperature-for-my-water-heater-1465372005>,
 548 2019.

549 [32] New York State Division of Housing and Community Renewal, Fact sheet 15: Heat and hot
550 water, <https://on.ny.gov/39vZ53M>, 2019.

551 [33] M. Booysen, J. Engelbrecht, M. Ritchie, M. Apperley, A. Cloete, How much energy can optimal
552 control of domestic water heating save?, Energy for Sustainable Development 51 (2019) 73 –
553 85.

554 [34] M. Roux, M. Apperley, M. J. Booysen, Comfort, peak load and energy: Centralised control of
555 water heaters for demand-driven prioritisation, Energy for Sustainable Development 44 (2018)
556 78 – 86.

557 [35] Consolidated Edison, Energy Efficiency and Demand Management Procedure: General Calculating
558 Customer Baseline Load, Specification EE-DR-01, <https://bit.ly/30Nfj4C>, 2020.

559 [36] New York Independent System Operator, Manual 7: Emergency demand response program,
560 <https://bit.ly/39uxGPx>, 2020.

561 [37] F. S. Goldner, Domestic hot water use study, multi-family building energy monitoring and
562 analysis for DHW system sizing criteria development, The Fairmont Press, Inc, United States,
563 1993.

564 [38] Time-of-Use Tariffs Innovation Landscaple Brief, International Renewable Energy Agency,
565 2019.